Electronic structure, Fermi surface, and antiferromagnetism of high-T_c cuprate materials and their doping dependence

M. Sugihara* and M. A. Ikeda
Department of Physics, College of Science and Engineering, Aoyama Gakuin University, Chitosedai 6-16-1, Setagaya-ku, Tokyo 157, Japan

P. Entel†
Theoretische Tieftemperaturphysik, Gerhard-Mercator-Universität-Gesamthochschule Duisburg, Lotharstraße 1, 47048 Duisburg, Germany

(Received 31 March 1997; revised manuscript received 25 August 1997)

We determine the electronic state of the antiferromagnetic CuO_2 layer of high-T_c cuprate materials on the basis of the three-band Hubbard model and derive the doping dependence of the antiferromagnetic order, electronic structure, and the Fermi surface. We solve the equation of motion for the single-electron Green's function taking into account the strong but finite Hubbard correlation and assuming the commensurate antiferromagnetic order. The result shows qualitatively correct behavior, i.e., the decline of the antiferromagnetic order along with the doping fraction of holes or electrons from the half-filled insulating phase. We also discuss the Fermi-surface structures dependent on the hole or electron doping fraction and compare these with the results of the angle-resolved photoemission spectroscopy. [S0163-1829(98)02217-6]

I. INTRODUCTION

Since the discovery of high-temperature superconductivity by Bednorz and Müller,[1] the abnormal physical properties found in the normal phase have stimulated theoretical physicists and have led to the creation of many new ideas.[2–4] It is generally accepted that the one-electron description breaks down in the insulating cuprate materials because of the large intra-atomic Coulomb repulsion U between d electrons on copper ions.[5]

We take our stand on the more conservative point of view and discuss the physics of a single CuO_2 layer on the basis of the two-dimensional, three-band Hubbard model.[6–8] The three-band Hubbard model has already been discussed in many theoretical works, however, only a few of them considered the presence of the antiferromagnetic (AF) order.[9,10] Recently, the results of angle-resolved photoemission spectroscopy (ARPES) seem to support the existence of antiferromagnetically nesting bands. In this context, it is important to inquire into details of the electronic band structure with the AF correlation. For that purpose, we propose a simple approach to obtain the electronic band structure of a single CuO_2 layer with the AF correlation between d electrons at copper sites. In the framework of the three-band Hubbard model, the most important effect of Hubbard correlation U can be treated exactly in the atomic limit and, for higher-order terms, we apply a decoupling procedure resembling the random-phase approximation. By these procedures, we can obtain the band structure, the energy dispersion, the spectral function, and the composition of copper and oxygen for the electronic states of the CuO_2 layer. The band structure depends on the average number of d electrons $\langle n_d \rangle$ and the AF order parameter $\langle s_Q \rangle$. These two parameters are determined self-consistently. The results show the AF parameter $\langle s_Q \rangle$ decreases with increasing doping fraction of holes or electrons. The tendency of decrease of $\langle s_Q \rangle$ is much more prominent for hole doping than for electron doping in qualitative agreement with experimental results. The existence of antiferromagnetism also affects the topology of the Fermi surface (FS). It is accepted that the cuprate materials have a large FS. Most of these ARPES experiments have been done on the metallic states,[11–13] but few have been done on the undoped AF compounds.[14] Abei *et al.*[15] performed ARPES experiments on $Bi_2Sr_2CaCu_2O_8$ (Bi2212) and found the structures that can be interpreted as the shadow bands that arise from the AF correlation. The three-band Hubbard model with AF order can explain the evolution of the FS obtained by ARPES. We discuss the evolution of the FS with doping of holes or electrons in detail in Sec. III.

II. THEORY

The undoped cuprate materials are AF insulators.[16–18] We propose a simple approach to obtain the electronic band structure of a single CuO_2 layer in the presence of the AF order. Due to the superexchange mechanism[19] mediated by the neighboring oxygen p_σ orbitals, the nearest-neighbor copper $d_{x^2-y^2}$ spins are coupled antiferromagnetically. Therefore, to investigate the effect of the AF order, it is sufficient to consider the three-band Hubbard model.

$$
\begin{aligned}
H=&\sum_{js}\ \varepsilon_d d_{js}^{\dagger} d_{js}+U\sum_{j}\ d_{j\uparrow}^{\dagger} d_{j\uparrow} d_{j\downarrow}^{\dagger} d_{j\downarrow}\\
&+\sum_{js}\ \varepsilon_\sigma(\sigma_{j+(a/2)s}^{\dagger}\sigma_{j+(a/2)s}+\sigma_{j+(b/2)s}^{\dagger}\sigma_{j+(b/2)s})\\
&-h\sum_{js}\ [d_{js}^{\dagger}(\sigma_{j+(a/2)s}-\sigma_{j+(b/2)s}-\sigma_{j-(a/2)s}+\sigma_{j-(b/2)s})\\
&+\text{H.c.}]-t\sum_{js}\ [\sigma_{j+(a/2)s}^{\dagger}(\sigma_{j+(b/2)s}-\sigma_{j-(b/2)s}\\
&-\sigma_{j+a+(b/2)s}+\sigma_{j+a-(b/2)s})+\text{H.c.}]. \qquad (1)
\end{aligned}
$$

The operators $d_{js}^{\dagger}$ and d_{js} ($\sigma_{j+(a/2)s}^{\dagger}$ and $\sigma_{j+(a/2)s}$) create and annihilate an electron with spin s in the copper $d_{x^2-y^2}$ (oxygen p_σ) orbital at site j ($j+a/2$), respectively. The Hubbard correlation energy on a copper ion is denoted by U. The nearest-neighbor copper-oxygen and oxygen-oxygen hybridizations are described by h and t, respectively. Orbital energies ε_d and ε_σ are measured from the chemical potential.

In the wave picture, we have

$$H=\sum_{ks}\varepsilon_d d_{ks}^{\dagger}d_{ks}+\frac{U}{N}\sum_{kk'q}d_{k\uparrow}^{\dagger}d_{k+q\uparrow}d_{k'+q\downarrow}^{\dagger}d_{k'\downarrow}+\sum_{ks}\varepsilon_\sigma(\sigma_{kxs}^{\dagger}\sigma_{kxs}+\sigma_{kys}^{\dagger}\sigma_{kys})-2ih\sum_{ks}[d_{ks}^{\dagger}(S_{kx}\sigma_{kxs}-S_{ky}\sigma_{kys})-\text{H.c.}]-4t\sum_{ks}S_{kx}S_{ky}(\sigma_{kxs}^{\dagger}\sigma_{kys}+\sigma_{kys}^{\dagger}\sigma_{kxs}), \tag{2}$$

where $S_{kx}=\sin k_x a/2$, $S_{ky}=\sin k_y a/2$.

To obtain the band structure of a single CuO_2 layer with the AF order, we use the Green's-function method. We use the following notation for the imaginary time-correlation function:

$$\langle\langle A;B^{\dagger}\rangle\rangle=-\langle T_\tau[A(\tau)B^{\dagger}(0)]\rangle=-\frac{\mathrm{Tr}\{e^{-\beta H}T_\tau[A(\tau)B^{\dagger}(0)]\}}{\mathrm{Tr}[e^{-\beta H}]}, \tag{3}$$

where $A(\tau)$ and $B^{\dagger}(\tau)$ are the Heisenberg operators, τ represents the imaginary time, and T_τ is the imaginary time-ordering operator. The equation of motion of the one-body Green's function $\langle\langle d_{k\uparrow};d_{k\uparrow}^{\dagger}\rangle\rangle$ is given by

$$-\frac{\partial}{\partial\tau}\langle\langle d_{k\uparrow};d_{k\uparrow}^{\dagger}\rangle\rangle=\delta(\tau)+\varepsilon_d\langle\langle d_{k\uparrow};d_{k\uparrow}^{\dagger}\rangle\rangle+\frac{U}{N}\sum_{k'q'}\langle\langle d_{k+q'\uparrow}d_{k'+q'\downarrow}^{\dagger}d_{k'\downarrow};d_{k\uparrow}^{\dagger}\rangle\rangle-2ihS_{kx}\langle\langle\sigma_{kx\uparrow};d_{k\uparrow}^{\dagger}\rangle\rangle+2ihS_{ky}\langle\langle\sigma_{ky\uparrow};d_{k\uparrow}^{\dagger}\rangle\rangle. \tag{4}$$

In Eq. (4), new Green's functions appear and it is necessary to establish the consistent treatment of the higher-order Green's function with a four d operator, in particular. We write down the equation of motion of the higher-order Green's function as follows:

$$\begin{aligned}-\frac{\partial}{\partial\tau}\sum_{k'q'}\langle\langle d_{k+q'\uparrow}d_{k'+q'\downarrow}^{\dagger}d_{k'\downarrow};d_{k\uparrow}^{\dagger}\rangle\rangle&=\delta(\tau)\sum_{k'q'}\langle\langle d_{k+q'\uparrow}d_{k'+q'\downarrow}^{\dagger}d_{k'\downarrow},d_{k\uparrow}^{\dagger}\rangle\rangle\\&+\varepsilon_d\sum_{k'q'}\langle\langle d_{k+q'\uparrow}d_{k'+q'\downarrow}^{\dagger}d_{k'\downarrow};d_{k\uparrow}^{\dagger}\rangle\rangle\\&+\frac{U}{N}\sum_{k'q'}\sum_{k''q''}\langle\langle d_{k+q'+q''\uparrow}d_{k'+q'\downarrow}^{\dagger}d_{k'\downarrow}d_{''+q''\downarrow}^{\dagger}d_{k''\downarrow};d_{k\uparrow}^{\dagger}\rangle\rangle\\&-2ih\sum_{k'q'}S_{k+q'x}\langle\langle\sigma_{k+q'x\uparrow}d_{k'+q'\downarrow}^{\dagger}d_{k'\downarrow};d_{k\uparrow}^{\dagger}\rangle\rangle\\&+2ih\sum_{k'q'}S_{k+q'y}\langle\langle\sigma_{k+q'y\uparrow}d_{k'+q'\downarrow}^{\dagger}d_{k'\downarrow};d_{k\uparrow}^{\dagger}\rangle\rangle\\&-2ih\sum_{k'q'}S_{k'x}\langle\langle d_{k+q'\uparrow}d_{k'+q'\downarrow}^{\dagger}\sigma_{k'x\downarrow};d_{k\uparrow}^{\dagger}\rangle\rangle\\&+2ih\sum_{k'q'}S_{k'y}\langle\langle d_{k+q'\uparrow}d_{k'+q'\downarrow}^{\dagger}\sigma_{k'y\downarrow};d_{k\uparrow}^{\dagger}\rangle\rangle\\&+2ih\sum_{k'q'}S_{k'+qx}\langle\langle d_{k+q'\uparrow}\sigma_{k'+q'x\downarrow}^{\dagger}d_{k'\downarrow};d_{k\uparrow}^{\dagger}\rangle\rangle\\&-2ih\sum_{k'q'}S_{k'+qy}\langle\langle d_{k+q'\uparrow}\sigma_{k'+q'y\downarrow}^{\dagger}d_{k'\downarrow};d_{k\uparrow}^{\dagger}\rangle\rangle.\end{aligned} \tag{5}$$

Here further higher-order Green's functions appear. The following identity,[20,21]

$$\frac{1}{N}\sum_{k'qk''q'}d_{k+q+q'\uparrow}d_{k'+q\downarrow}^{\dagger}d_{k'\downarrow}d_{k''+q'\downarrow}^{\dagger}d_{k''\downarrow}=\sum_{k'q}d_{k+q\uparrow}d_{k'+q\downarrow}^{\dagger}d_{k'\downarrow}, \tag{6}$$

which is equivalent to the Pauli principle (see Appendix), is applied to the term involving the correlation energy U. By using this identity we can replace the third term in the right-hand side of Eq. (5) as follows:

$$\frac{U}{N}\sum_{k'q'}\sum_{k''q''}\langle\langle d_{k+q'+q''\uparrow}d_{k'+q'\downarrow}^{\dagger}d_{k'\downarrow}d_{k''+q''\downarrow}^{\dagger}d_{k''\downarrow};d_{k\uparrow}^{\dagger}\rangle\rangle=U\sum_{k'q'}\langle\langle d_{k+q'\uparrow}d_{k'+q'\downarrow}^{\dagger}d_{k'\downarrow};d_{k\uparrow}^{\dagger}\rangle\rangle. \tag{7}$$

In Eq. (5), there remain other types of Green's functions with one σ operator. We use the random-phase approximation (RPA) for them, i.e.,

$$\langle\langle\sigma_{k+q'x\uparrow}d_{k'+q'\downarrow}^{\dagger}d_{k'\downarrow};d_{k\uparrow}^{\dagger}\rangle\rangle\simeq\langle d_{k'+q'\downarrow}^{\dagger}d_{k'\downarrow}\rangle\times\langle\langle\sigma_{k+q'x\uparrow};d_{k\uparrow}^{\dagger}\rangle\rangle. \tag{8}$$

Here, we assume the commensurate AF order,

$$\langle d_{j\uparrow}^{\dagger}d_{j\uparrow}\rangle+\langle d_{j\downarrow}^{\dagger}d_{j\downarrow}\rangle=\langle n_d\rangle, \tag{9}$$

$$\langle d_{j\uparrow}^{\dagger}d_{j\uparrow}\rangle-\langle d_{j\downarrow}^{\dagger}d_{j\downarrow}\rangle=\langle s_Q\rangle e^{-iQR_j}. \tag{10}$$

$\langle n_d\rangle$ is the average number of electrons in a copper $d_{x^2-y^2}$ orbital and $\langle s_Q\rangle$ is the mean staggered magnetization. Q is the AF wave vector

$$Q=\left(\frac{\pi}{a},\frac{\pi}{a}\right). \tag{11}$$

Using the relations (9) and (10), the expectation value $\Sigma_k\langle d_{k+q\downarrow}^{\dagger}d_{k\downarrow}\rangle$ can be replaced by[22,23]

$$\frac{1}{N}\sum_k \langle d^\dagger_{k+q\downarrow} d_{k\downarrow}\rangle = \frac{1}{N}\sum_j \langle d^\dagger_{j\downarrow} d_{j\downarrow}\rangle e^{-iqR_j}$$

$$= \left[\delta_{q,0}\frac{\langle n_d\rangle}{2} - \delta_{q,Q}\frac{\langle s_Q\rangle}{2}\right]. \quad (12)$$

The same average value (12) is also used for the term $\langle \Sigma_{k'q'}(d_{k+q'\uparrow} d^\dagger_{k'+q'\downarrow} d_{k'\downarrow}, d^\dagger_{k\uparrow})\rangle$ in Eq. (5). By this procedure, the equation of motion (5) for the higher-order Green's function is reduced to

$$\left[-\frac{\partial}{\partial\tau} - (\varepsilon_d + U)\right]\sum_{k'q'} \langle\langle d_{k+q'\uparrow} d^\dagger_{k'+q'\downarrow} d_{k'\downarrow}; d^\dagger_{k\uparrow}\rangle\rangle$$

$$= \delta(\tau) N \frac{\langle n_d\rangle}{2} - 2ihN\frac{\langle n_d\rangle}{2} S_{kx}\langle\langle \sigma_{kx\uparrow}; d^\dagger_{k\uparrow}\rangle\rangle$$

$$+ 2ihN\frac{\langle s_Q\rangle}{2} S_{k+Qx}\langle\langle \sigma_{k+Qx\uparrow}; d^\dagger_{k\uparrow}\rangle\rangle$$

$$+ 2ihN\frac{\langle n_d\rangle}{2} S_{ky}\langle\langle \sigma_{ky\uparrow}; d^\dagger_{k\uparrow}\rangle\rangle$$

$$- 2ihN\frac{\langle s_Q\rangle}{2} S_{k+Qy}\langle\langle \sigma_{k+Qy\uparrow}; d^\dagger_{k\uparrow}\rangle\rangle. \quad (13)$$

Thus, the hierarchy of equations is truncated to a closed set of equations of motion.

Fourier transformation in the imaginary time is defined by

$$\langle\langle A; B^\dagger\rangle\rangle = \frac{1}{\beta}\sum_{\omega_n} e^{-i\omega_n\tau}\langle\langle A; B^\dagger\rangle\rangle_{\omega_n}, \quad (14)$$

where ω_n is Matsubara frequency for fermions: $\omega_n = \pi/\beta(2n+1)$, $(n=0,\pm1,\pm2,\ldots)$. Fourier components of the Green's functions generally have the form

$$\langle\langle A; B^\dagger\rangle\rangle_{\omega_n} = \frac{\text{Numerator}(i\omega_n)}{\text{Denominator}(i\omega_n)}. \quad (15)$$

The denominator is common to all of the Green's functions, and is a polynomial of 8th order in the frequency $i\omega_n$. The roots for the equation, Denominator $(i\omega_n)=0$, give the eight energy eigenvalues at each k point. The numerator of each Green's function determines the spectral weight of each band. We use the numerical parameters as follows: $\varepsilon_\sigma - \varepsilon_d = 3.5$, $U=8.8$, $h=1.3$, and $t=0.7$ (eV).[21,24,25] We can determine $\langle n_d\rangle$ and $\langle s_Q\rangle$ self-consistently by the following equations:

$$\langle n_d\rangle = \frac{1}{\beta N}\sum_{k<k_F}\sum_{\omega_n}\left[\langle\langle d_{k\uparrow}; d^\dagger_{k\uparrow}\rangle\rangle_{\omega_n} + \langle\langle d_{k\downarrow}; d^\dagger_{k\downarrow}\rangle\rangle_{\omega_n}\right],$$

$$\langle s_Q\rangle = \frac{1}{\beta N}\sum_{k<k_F}\sum_{\omega_n}\left[\langle\langle d_{k+Q\uparrow}; d^\dagger_{k\uparrow}\rangle\rangle_{\omega_n} - \langle\langle d_{k+Q\downarrow}; d^\dagger_{k\downarrow}\rangle\rangle_{\omega_n}\right]. \quad (16)$$

III. RESULTS AND DISCUSSION

From the coupled conditions (16), we determine the self-consistent combinations of $\langle n_d\rangle$ and $\langle s_Q\rangle$. The dependence of the AF order $\langle s_Q\rangle$ on $\langle n_d\rangle$ in Fig. 1, shows a kink at $\langle n_d\rangle = 1.31$. $\langle s_Q\rangle$ decreases for both sides when $\langle n_d\rangle$ deviates from the peak value. In our interpretation, the maximum $\langle s_Q\rangle$ corresponds to the undoped phase, but the total electron number below the Fermi level at the peak value is 5.077 and unfortunately there is a 1.51% discrepancy between our calculated total number and the exact half-filled number, 5.000. We consider, however, that the deviation $1/N\Sigma_{k<k_F,s}[\langle n_{kds}\rangle + 2\langle n_{k\sigma s}\rangle] - 5.077 = x$ gives the doping fraction, hole doping for $x<0$, and electron doping $x>0$. Here, $\langle n_{kds}\rangle$ and $\langle n_{k\sigma s}\rangle$ are the d- and σ-electron components calculated numerically for each band. The AF correlation decreases for both hole and electron doping in qualitative agreement with the experimental facts. The asymmetry of decrease of $\langle s_Q\rangle$ between hole and electron doping is apparent. Quantitatively, the AF order vanishes at $|x| = 0.074$ for hole doping and $x=0.22$ for electron doping and these values are larger than the measured values $|x|=0.015$ for $La_{2-x}Sr_xCuO_4$ (Ref. 26) and $x=0.14$ for $Nd_{2-x}Ce_xCuO_4$ (NCCO).[27] These quantitative disagreements are not surprising, since we could not take into account the effect of the AF fluctuations in this calculation. It must be stressed that the undoped phase does not correspond to $\langle n_d\rangle = 1.0$ in our model, because of the hybridization between oxygen p_σ.

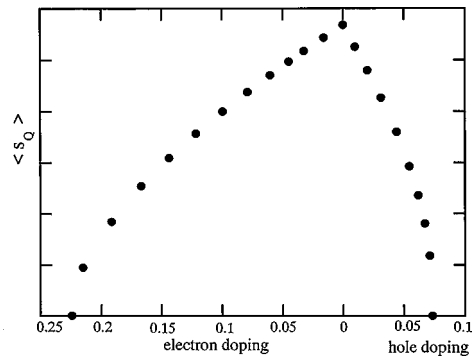

FIG. 1. The doping dependence of the antiferromagnetic (AF) order $\langle s_Q\rangle$.

The asymmetry of the AF phase between hole and electron doping has been discussed by several authors.[9,10,28,29] Most of them, however, are based on the t-J model.[28,29] The t-J model has the electron-hole symmetry and in order to describe the asymmetric behavior of the AF stability, one must extend the t-J model to the t-t'-J model, which includes the next-nearest-neighbor hopping amplitude t', and the electron-hole asymmetry arises from the sign of the hopping amplitude t'. On the other hand, the three-band Hubbard model has the inherent electron-hole asymmetry and it offers a good starting point to describe the asymmetric AF behavior of cuprates.

Zhang and co-workers[9] discussed the AF order by the three-band Hubbard model but they treated the Hubbard correlation U by the slave boson method in the limit $U\to\infty$. There are very few works that discuss the AF stability within the finite U model. One such article is by Fedro *et al.*[10] They have applied the projection-operator method to the three-band Hubbard model with a finite U value and have also shown the diminution of the AF order with doping of holes or electrons, but the discrepancy between the doping concentration and the observed value is larger than in our results.

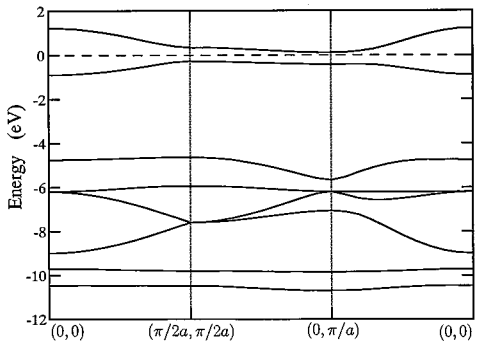

FIG. 2. Band structure of the AF CuO_2 layer described by the three-band Hubbard model with $\langle n_d \rangle = 1.31$ and $\langle s_Q \rangle = 0.568$. The Fermi level is located between the two antiferromagnetically split upper-Hubbard bands and represented by the broken line.

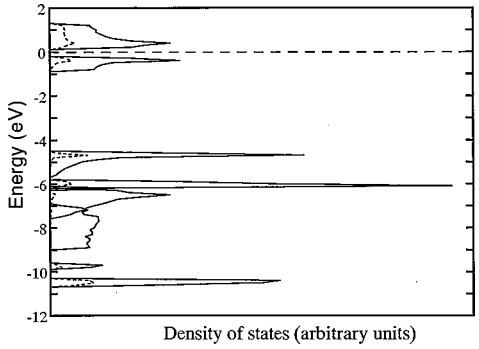

FIG. 3. The density of states of the AF three-band Hubbard model with the same values of parameters $\langle n_d \rangle$ and $\langle s_Q \rangle$ as in Fig. 2. The highest two bands and the lowest two bands are mainly of copper origin, and mainly oxygen bands are formed between them. Each band also includes the minority component, through the hybridization h, and the rate of the minority component is represented by broken lines.

From each of the self-consistent combinations $\langle n_d \rangle$ and $\langle s_Q \rangle$, we can determine the electronic band dispersions and the d- and σ-component density of states of the CuO_2 layer. Figure 2 shows the band structure for the undoped insulating phase at the maximum AF order ($\langle n_d \rangle = 1.31$ and $\langle s_Q \rangle = 0.568$), shown along the high symmetry lines $(0,0) - (\pi/2a, \pi/2a) - (\pi/a, 0) - (0,0)$ in the Brillouin zone. The Fermi energy, shown as the dashed line, and taken as the origin 0 of the energy axis, is located between the two upper-Hubbard bands that are split by the AF order. The lowest two bands correspond to the antiferromagnetically split lower-Hubbard bands. Four bands between the upper- and lower-Hubbard bands have mainly oxygen character. In our band structure there are two kinds of gaps. One is the Hubbard gap between the upper-Hubbard and the oxygen bands. The other is the small gap between the antiferromagnetically split upper-Hubbard bands. The AF gap is also seen between the lower-Hubbard bands. The charge-transfer gap (CT gap) can be observed by the optical reflection. The small AF gap has not yet been observed and this seems to be a drawback of this paper. We shall add a comment at the end of the concluding section on this point.

In the band structure, there exists a flat band near the Fermi level, which has been observed by ARPES (Refs. 11–13) and is in agreement with other theoretical calculations.[30–33] Figure 3 shows the density of states for the undoped insulating AF phase corresponding to Fig. 2. The solid lines show the total density. Broken lines for each band show the minority component, i.e., oxygen, for the upper- and lower-Hubbard bands, copper for the four oxygen bands between them. Figure 3 shows that the AF split upper-Hubbard bands include not only the copper component, but also an appreciable fraction of the oxygen component. This represents the effect of hybridization between copper and oxygen. The following fact must be noted: although most of the holes are doped in the upper-Hubbard band, a finite fraction of doped carriers occupies the oxygen sites.

Figure 4 indicates the characters of the doped carriers. The abscissa is the concentration of doped holes or electrons. The solid triangles and the solid diamonds represent the concentrations of copper and oxygen characters, respectively. The solid circles are the total number of doping carriers. The open marks indicate those calculated in the paramagnetic (PM) phase,[7] which describes the overdoped regions. Although the rate of doped holes with oxygen character slightly decreases in the PM phase, there is no discontinuity of concentrations between the AF and the PM phases. It should be remarked that nearly 50% of doped holes have oxygen character and a large number of doped electrons have copper character. This disparity reflects the quantitatively different doping dependences of the AF order between hole and electron doping. Since added carriers with oxygen character strongly suppress the AF exchange interaction between copper atoms, the AF order is destroyed. In the case of electron doping, the character of carriers is predominantly of copper, therefore the superexchange interaction remains almost the same. The spin magnetic moment of copper ions decreases instead, and this is the reason for the rather weak decrease of the AF order in the electron doped materials. Therefore, the quantitative difference can be explained by the different ratio of doped carrier characters and is supported by experimental observations,[34,35] qualitatively.

The FS topology gives an important clue for the investigation of the electronic structure of cuprate materials.

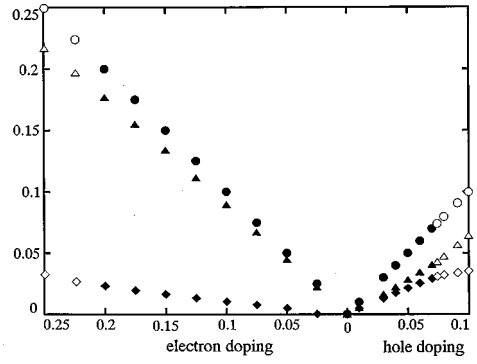

FIG. 4. The rate of characters of doped carriers. The abscissa is the concentration of doped holes or electrons. The solid triangles and the solid diamonds show carrier concentrations of copper and oxygen characters, respectively. The solid circles correspond to the total numbers of doping carriers. The open marks indicate those calculated in the paramagnetic (PM) three-band Hubbard model. Although the doped holes occupy the upper Hubbard band, the mixing oxygen rate reaches up to 50%. On the other hand, the doped electrons have an almost copper character.

ARPES experiments seem to provide evidence for a large FS, (Refs. 11–13) but these experiments have been done on metallic samples. On the other hand, there is an assertion that the spectra obtained on insulating samples support the small hole pockets.[14] And from the experiments on the weakly doped $Sr_2CuO_2Cl_2$, Wells *et al.*[36] expect that for very low doping levels the copper oxides must have a small pocket FS. Recently, Abei *et al.*[15] have reported the presence of a shadow band due to the AF order and the existence of features similar to hole pockets in Bi2212, which is consistent with transport and optical data.[37,38] The PM Hubbard model cannot reproduce the small pocket FS centered around $(\pi/2a,\pi/2a)$.[39] However, the presence of the AF order of copper atoms changes the topology of the FS drastically. The FS calculated by the AF three-band Hubbard model is shown in Figs. 5(a)–5(d). At a very low hole density FS starts with hole pockets centered at $(\pi/2a,\pi/2a)$ [Fig. 5(a)]. The pockets grow along the $(0,\pi/a)-(\pi/a,0)$ directions [Figs. 5(b) and 5(c)] with an increasing fraction of doped holes. Finally, at high doping levels they evolve into a standard circular FS with phase transition between the AF and the PM states [Fig. 5(d)]. The corresponding band structures are given in Figs. 6(a)–6(d). In Fig. 6(d), the band structure is shown by the enlarged PM Brillouin zone. At a small hole doping level, the evolution with doping of the FS is similar to the results obtained by the t-J model[40,41] and the AF one-band Hubbard model.[42]

In a heavily doped case, the FS obtained by us in the PM state has a diamond shape with rounded corners with the center at (0,0) and the band crosses the Fermi level between $(\pi/a,0)$ and (0,0). But the observed FS by the ARPES (Refs. 11–13) in metallic phases has the center at each corner of the Brillouin zone, i.e., $(\pm\pi/a,\pm\pi/a)$ and $(\pm\pi/a,\mp\pi/a)$, and looks very different from our result. This discrepancy seems to be closely related to the slow decrease of the AF order in our result. If the decrease of the AF order were more rapid, the band would cross the Fermi level between $(\pi/a,0)$ and $(\pi/a,\pi/a)$ and the FS of the metallic state would enclose the corners of the Brillouin zone in accord with the experimental observations.

Next, we deal with the topological evolution of the FS with electron doping. The change of the FS with electron doping is depicted in Figs. 7(a)–7(d) and the corresponding band structures are given in Figs. 8(a)–8(d). The doped electrons at first occupy the space around $(\pi/a,0)$ [Fig. 7(a)] and the behavior of the growth of the electron pockets is different from the hole doping case [Figs. 7(b) and 7(c)]. In these figures, the dotted regions are occupied by doped electrons. Due to the AF order, the two upper-Hubbard bands have weak dispersion along $(\pi/2a,\pi/2a)-(\pi/a,0)$ line. Because of the declination of the two upper-Hubbard bands, the topological evolution of the FS is different between hole and electron doping. The ARPES have shown that the topological development of NCCO seems to be different from hole doped materials.[43] The FS observed in metallic states has the large electron pockets around $(\pi/a,\pi/a)$ and its shape agrees with our result represented by Fig. 7(d). If the decrease of the AF order were more rapid in accord with the experimental results, the FS of the PM state would shrink without the change in its shape.

The flat bands in our band structures need to be men-

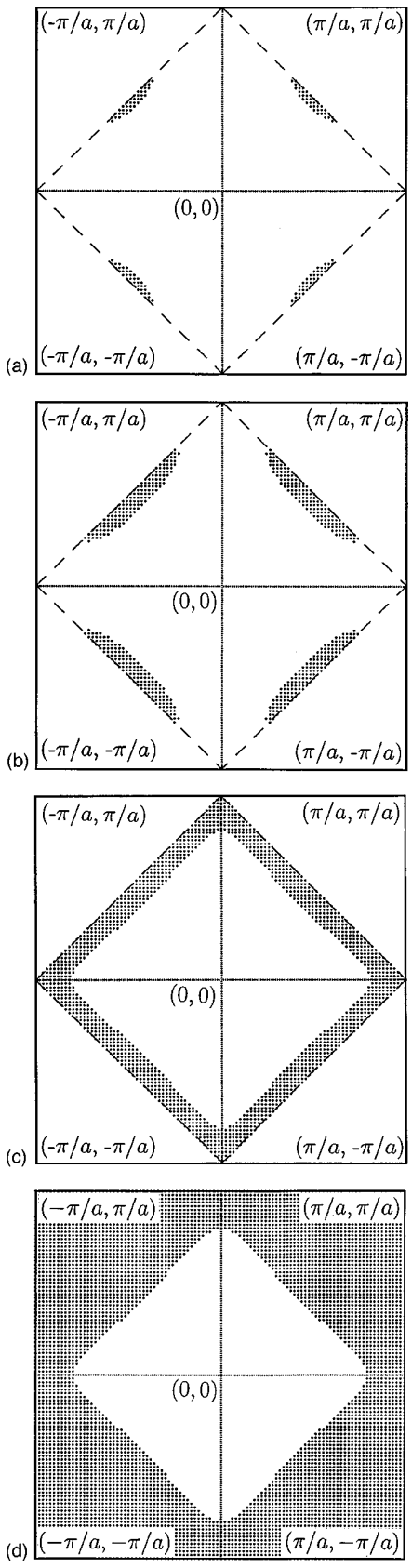

FIG. 5. Fermi surface (FS) of the AF three-band Hubbard model. Dotted regions are the Fermi surface (FS) of the AF three-band Hubbard model. Dotted regions are occupied by holes: (a) $x=0.01$, (b) $x=0.03$, (c) $x=0.07$, (d) $x=0.074$. (d) is calculated by the PM three-band Hubbard model.

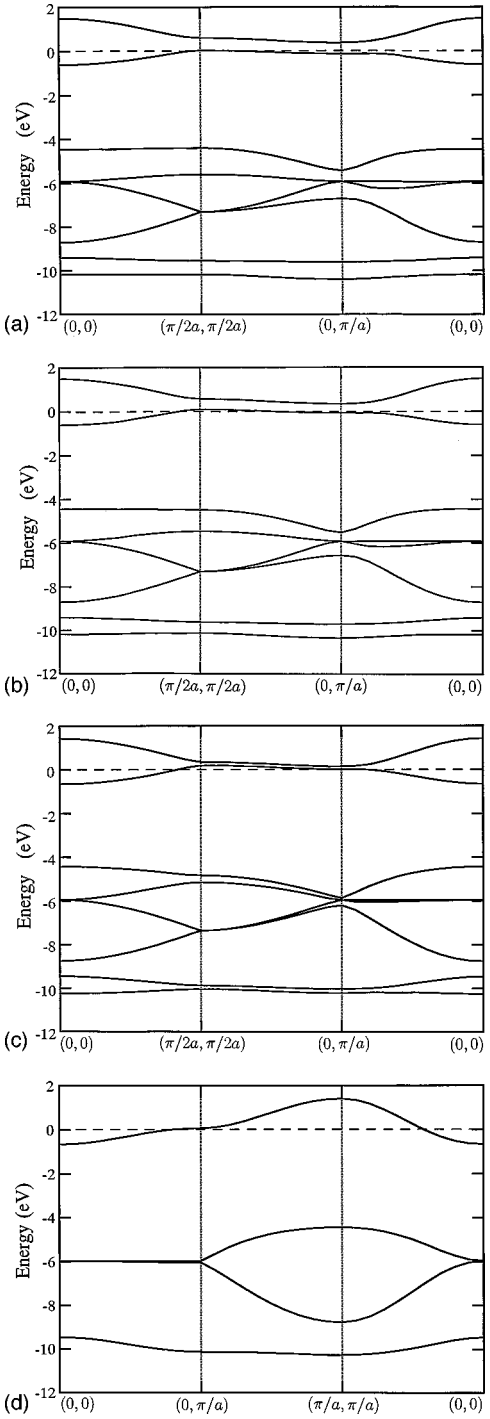

FIG. 6. Band structures (a)–(c) show the AF three-band Hubbard models that correspond to Figs. 5(a)–5(c). (d) is calculated by the three-band Hubbard model in the PM phase in correspondence with Fig. 5(d) and is represented by the enlarged PM Brillouin zone.

tioned. The flat bands are considered to play significant roles in the physical properties (transport phenomena, superconductivity, etc.) of cuprate materials.[44–46] Beenen and Edwards[31] have applied Roth's two-pole approximation to the one-band Hubbard model and their results agree remarkably well with the Monte Carlo results.[32] Their results show the existence of a flat band below the Fermi level in the half-filled case. With hole doping, there is also an additional broad bump near $(\pi/a, \pi/a)$ where doped holes are seen and

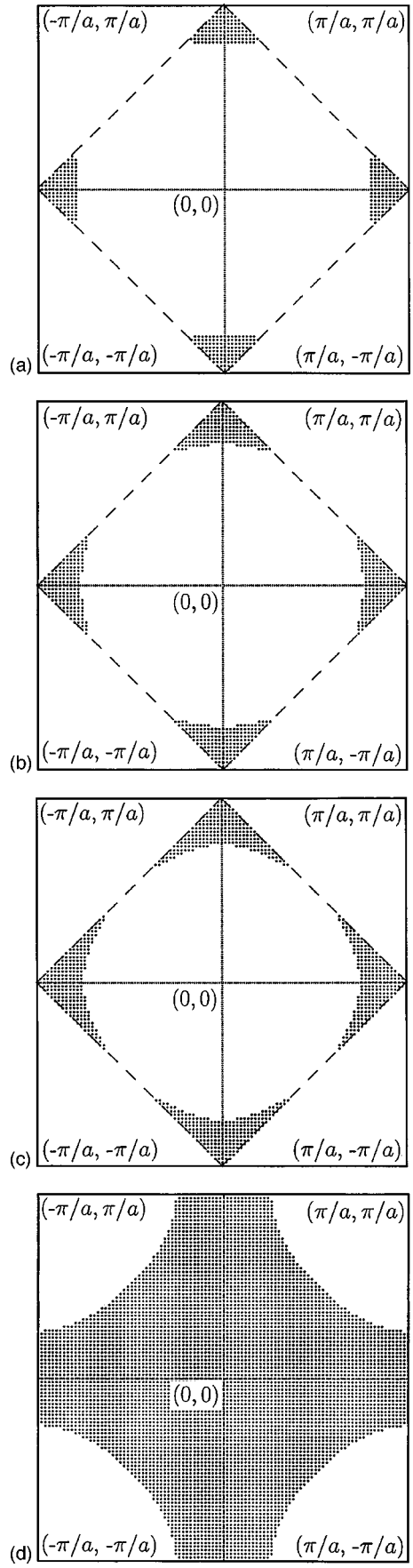

FIG. 7. FS of the AF three-band Hubbard model. Dotted regions are occupied by electrons. (a) $x=0.10$, (b) $x=0.15$, (c) $x=0.20$, (d) $x=0.22$. (d) is calculated by the PM three-band Hubbard model.

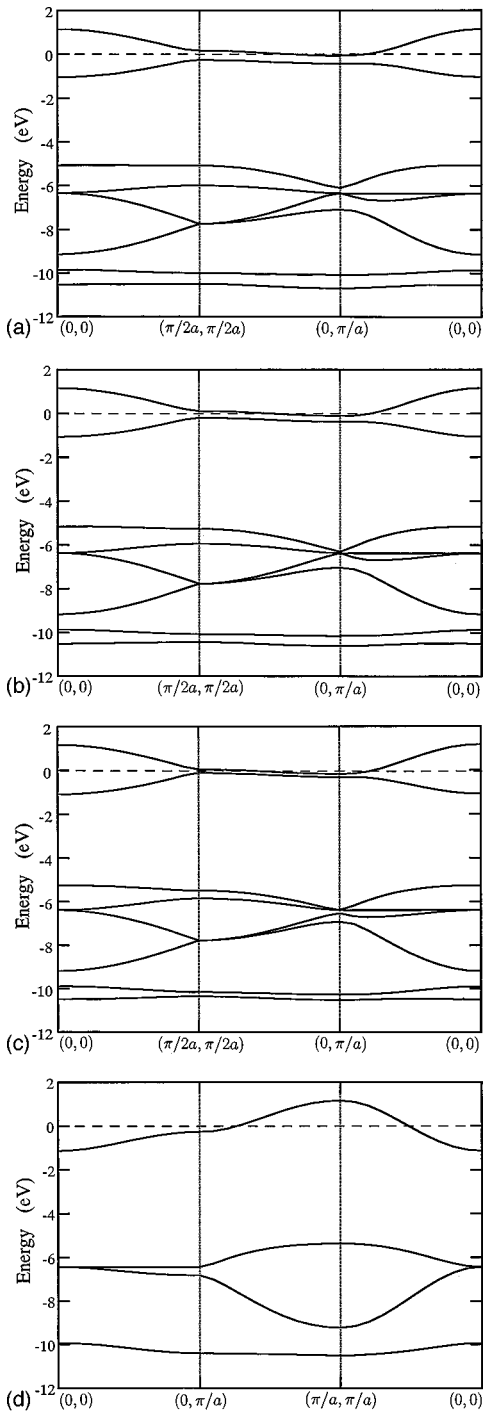

FIG. 8. Band structures (a)–(c) show the AF three-band Hubbard models that correspond to Figs. 7(a)–7(c). (d) is calculated by the PM three-band Hubbard model in correspondence with Fig. 7(d) and is represented by the enlarged PM Brillouin zone.

the band is still dispersionless in the vicinity of $(\pi/a,0)$ and stays near the Fermi level.

We can explain the behavior of the flat bands by the three-band Hubbard model with AF order, but the scenario is different from the one-band Hubbard model. In our results for the half-filled case, the flat bands are located below the Fermi level (Fig. 1). From Figs. 6(a)–6(c), we notice that the flat bands still exist near the Fermi level in the hole doping case. After transition from the AF state to the PM state, the upper-Hubbard band has dispersion, but at $(\pi/a,0)$ we can find a flat region [Fig. 6(d)]. Recently, Marshall *et al.*[47] have shown a radical change of the electronic structure around $(\pi/a,0)$ in Bi2212. As the rate of hole doping increases, the Fermi level approaches the flat band. In our results, although the change of the band around $(\pi/a,0)$ is not so drastic, it seems to agree with these experiments, at least qualitatively. In the electron doping case, there is also a dispersionless band below the Fermi level [Figs. 8(a)–8(c)]. It is obvious from Fig. 8(d) of the PM case that the flat band exists only at $(\pi/a,0)$ and still stays below the Fermi level. Experiments show a clearly different location of the flat band between the hole doped and the electron doped materials.[48] In NCCO, the flat band is approximately 300 meV below the Fermi level, while in the hole doped materials it is located very close to the Fermi level. The location of the flat region in our band structures agrees with the experimental observations for both hole [Fig. 6(d)] and electron [Fig. 8(d)] doped cases.

IV. CONCLUSIONS

We have calculated the AF order $\langle s_Q \rangle$ and its doping dependence by the three-band Hubbard model of a single CuO_2 layer. We have reproduced the decrease of $\langle s_Q \rangle$ with doping fraction of holes or electrons (Fig. 1) in qualitative agreement with other experiments. The asymmetry of the decrease of Néel temperature between hole and electron doped materials can be reasonably interpreted by the nature of the doped carriers (Fig. 2). On the evolution of FS with hole doping, we have obtained good agreement with the recent ARPES experiments. For electron doped materials, the FS and its evolution we obtained are different from the results for hole doped materials. For electron doped materials, experiments have been carried out only for the metallic materials, but the evolution of the FS seems to be different from the results for hole doped materials. We hope ARPES experiments on NCCO for very low doping levels will be carried out in the future. Concerning the flat band, although there are several theoretical interpretations, our results differ from them and seem to agree with experiments which show a different position with respect to the Fermi level between hole doped and electron doped materials. In this paper, we have calculated normal-state properties of a single CuO_2 layer. We think that the results such as those shown in the magnetic phase diagram and topologies of the FS are relevant for high-T_c copper oxide materials.

An apparent drawback of the results of this paper is that the Fermi level in the undoped phase lies in the AF gap that is formed in the upper-Hubbard band and not in the CT gap as is generally believed and also suggested by experiments such as optical reflection. Readers may get the impression that this result shows the defect of the approximation used in this paper. We cannot agree with this view. The method is based on the identity (6) and the only approximation is a kind of RPA, typically Eq. (8), in decoupling the set of equations of motion, applied to terms that arise from the hybridization h in the second stage equation, i.e., the last six terms in Eq. (5). We believe that using the approximation does not undermine the validity of our results. Further, we have to remark that the split bands have a quite different character from the AF split bands of the itinerant electron picture.

While the upper band has almost purely d character, the lower band is composed of the strongly d-p hybridized electrons, and especially near the region around $(\pi/2a,\pi/2a)$, where the Fermi surface appears at the lowest hole doping levels, the mixing oxygen rate reaches up to 50%.

On the other hand, nuclear quadrupole resonance experiments[49] have shown that nearly 20% of $d_{x^2-y^2}$ orbitals are doubly occupied by electrons. This has also been verified by the numerical calculations by Ohota and co-workers[50] and Tsuji and co-workers[51] for the half filled and low doping region. This means that the Fermi level crosses the upper Hubbard band of the $d_{x^2-y^2}$ orbital and we cannot describe simply the cuprates by the Brinkman-Rice type metal-insulator transition.[52] We think that the location of the Fermi level obtained in this paper for the undoped case conforms with this view.

However, we think the serious defect in our theory is that we could not take into account the effect of AF spin fluctuations. We have determined AF order and the chemical potential self-consistently. In order to be truly self-consistent, however, we have to include the effect of spin fluctuations around the AF ordered state, but we could not do that in this paper. If we could take into account the effect of the spin fluctuation, the reduction of the AF order would tend to become more rapid, and the description of the electronic states around the doping region near to $T_N \sim 0$ would change.

Note added in proof. Marshall *et al.* have carried out ARPES experiments on insulating Bi2212 materials and shown the AF nested band around $(\pi/2a,\pi/2a)$ (Ref. 47, Fig. 3). In Fig. 2 we plotted the band structure for the undoped insulating phase by the AF reduced Brillouin zone. If we plot it by the enlarged PM Brillouin zone, the AF nested band similar to their experimental results is obtained. We think the experimental results by Marshall *et al.* support the existence of the AF nested band near the Fermi level.

APPENDIX: PROOF OF THE IDENTITY (6)

Here, we show the proof of the identity (6). Remarking that the Fourier transform of the number operator is given by

$$\sum_J e^{iqR_J} d_{Js}^\dagger d_{Js} = \sum_k d_{k+qs}^\dagger d_{ks},$$

we have

$$\begin{aligned}
&\sum_{k'qk''q'} d_{k+q+q'\uparrow} d_{k'+q\downarrow}^\dagger d_{k'\downarrow} d_{k''+q'\downarrow}^\dagger d_{k''\downarrow} \\
&= \frac{1}{\sqrt{N}} \sum_{qq'} \sum_{IJJ'} e^{-i(k+q+q')R_I} d_{I\uparrow} e^{iqR_J} n_{J\downarrow} e^{iq'R_{J'}} n_{J'\downarrow} \\
&= \frac{N^2}{\sqrt{N}} \sum_I e^{-ikR_I} d_{I\uparrow} n_{I\downarrow} n_{I\downarrow} = \frac{N^2}{\sqrt{N}} \sum_I e^{-ikR_I} d_{I\uparrow} n_{I\downarrow} \\
&= N \sum_{k'q} d_{k+q\uparrow} d_{k'+q\downarrow}^\dagger d_{k'\downarrow}.
\end{aligned}$$

We used the Pauli principle $n_{I\downarrow}^2 = n_{I\downarrow}$.

*Electronic address: sugihara@phys.aoyama.ac.jp
†Electronic address: entel@thp.uni-duisburg.de

[1] J. G. Bednorz and K. A. Müller, Z. Phys. B **64**, 189 (1986).
[2] P. W. Anderson, Science **235**, 1196 (1987).
[3] N. Nagaosa and P. A. Lee, Phys. Rev. Lett. **64**, 2450 (1990).
[4] S.-C. Zhang, Science **275**, 1089 (1997).
[5] There are many good reviews, for example, A. P. Kampf, Phys. Rep. **249**, 219 (1994); W. Brenig, *ibid.* **251**, 153 (1995); E. Dagotto, Rev. Mod. Phys. **66**, 763 (1994).
[6] V. J. Emery, Phys. Rev. Lett. **58**, 2794 (1987).
[7] P. Entel and J. Zielinski, Phys. Rev. B **42**, 307 (1990).
[8] P. Unger and P. Fulde, Phys. Rev. B **48**, 16 607 (1993).
[9] W. Zhang, M. Avignon, and K. H. Bennemann, Phys. Rev. B **42**, 10 192 (1990).
[10] A. J. Fedro, Yu Zhou, T. C. Leung, B. N. Harmon, and S. K. Sinha, Phys. Rev. B **46**, 14 785 (1992).
[11] J. C. Campuzano, G. Jennings, M. Faiz, L. Beaulaigue, B. W. Veal, J. Z. Liu, A. P. Paulikas, K. Vandervoort, H. Claus, R. S. List, A. J. Arko, and R. J. Bartlett, Phys. Rev. Lett. **64**, 2308 (1990).
[12] D. M. King, Z.-X. Shen, D. S. Dessau, D. S. Marshall, C. H. Park, W. E. Spicer, J. L. Peng, Z. Y. Li, and R. L. Greene, Phys. Rev. Lett. **73**, 3298 (1994).
[13] K. Gofron, J. C. Campuzano, A. A. Abrikosov, M. Lindroos, A. Bansil, H. Ding, D. Koelling, and B. Dabrowski, Phys. Rev. Lett. **73**, 3302 (1994).
[14] R. Liu, B. W. Veal, A. P. Paulikas, J. W. Downey, P. J. Kostić, S. Fleshler, U. Welp, C. G. Olson, X. Wu, A. J. Arko, and J. J. Joyce, Phys. Rev. B **46**, 11 056 (1992).
[15] P. Abei, J. Osterwalder, P. Schwaller, L. Schlapbach, M. Shimada, T. Mochiku, and K. Kadowaki, Phys. Rev. Lett. **72**, 2757 (1994).
[16] D. Vaknin, S. K. Sinha, D. E. Moncton, D. C. Johnston, J. M. Newsam, C. R. Safinya, and H. E. King, Jr., Phys. Rev. Lett. **58**, 2802 (1987).
[17] J. M. Tranquada, D. E. Cox, W. Kunnmann, H. Moudden, G. Shirane, M. Suenaga, P. Zolliker, D. Vaknin, S. K. Sinha, M. S. Alvarez, A. J. Jacobson, and D. C. Johnston, Phys. Rev. Lett. **60**, 156 (1988).
[18] G. M. Luke, B. J. Sternlieb, Y. J. Uemura, J. H. Brewer, R. Kadono, R. F. Kiefl, S. R. Kreitzman, T. M. Riseman, J. Gopalakrishnan, A. W. Sleight, M. A. Subramanian, S. Uchida, H. Takagi, and Y. Tokura, Nature (London) **338**, 49 (1989).
[19] P. W. Anderson, Phys. Rev. **115**, 2 (1959).
[20] M. A. Ikeda, U. Larsen, and R. D. Mattuck, Phys. Lett. **39A**, 55 (1972).
[21] M. Sugihara, K. Numai, Y. Nakao, Y. Kikuchi, and M. A. Ikeda, Physica C **214**, 159 (1993).
[22] J. R. Schrieffer, X. G. Wen, and S. C. Zhang, Phys. Rev. B **39**, 11 663 (1989).
[23] M. Sugihara, T. Nakayama, A. Tanabe, and M. A. Ikeda, Phys. Lett. A **221**, 400 (1996).
[24] M. S. Hybertsen, M. Schlüter, and N. E. Christensen, Phys. Rev. B **39**, 9028 (1989).
[25] H. Eskes and G. A. Sawatzky, Phys. Rev. B **44**, 9656 (1991).
[26] B. Keimer, N. Belk, R. J. Birgeneau, A. Cassanho, C. Y. Chen, M. Greven, M. A. Kastner, A. Aharony, Y. Endoh, R. W. Erwin, and G. Shirane, Phys. Rev. B **46**, 14 034 (1992).

[27] G. M. Luke, L. P. Le, B. J. Sternlieb, Y. J. Uemura, J. H. Brewer, R. Kadone, R. F. Kiefl, S. R. Kreitzman, T. M. Riseman, C. E. Stronach, M. R. Davis, S. Uchida, H. Takagi, Y. Tokura, Y. Hidaka, T. Murakami, J. Gopalakrishnan, A. W. Sleight, M. A. Subramanian, E. A. Early, J. T. Markert, M. B. Maple, and C. L. Seaman, Phys. Rev. B **42**, 7981 (1990).

[28] T. Toyama and S. Maekawa, Phys. Rev. B **49**, 3596 (1994).

[29] R. J. Gooding, K. J. E. Vos, and P. W. Leung, Phys. Rev. B **50**, 12 866 (1994).

[30] V. Zlatić, P. Entel, and S. Grabowski, Europhys. Lett. **34**, 693 (1996).

[31] J. Beenen and D. M. Edwards, Phys. Rev. B **52**, 13 636 (1995).

[32] N. Bulut, D. J. Scalapino, and S. R. White, Phys. Rev. B **50**, 7215 (1994); Phys. Rev. Lett. **73**, 748 (1994).

[33] G. Dopf, J. Wagner, P. Dieterich, A. Muramatsu, and W. Hanke, Phys. Rev. Lett. **68**, 2082 (1992).

[34] Z.-X. Shen, J. W. Allen, J. J. Yek, J.-S. Kang, W. Ellis, W. Spicer, I. Lindau, M. B. Maple, Y. D. Dalichaouch, M. S. Torikachvili, J. Z. Sun, and T. H. Geballe, Phys. Rev. B **36**, 8414 (1987).

[35] M. Alexander, H. Romberg, N. Nücker, P. Adelmann, J. Fink, J. T. Markert, M. B. Maple, S. Uchida, H. Takagi, Y. Tokura, A. C. W. P. James and D. W. Murphy, Phys. Rev. B **43**, 333 (1991).

[36] B. O. Wells, Z.-X. Shen, A. Matsuura, D. M. King, M. A. Kastner, M. Greven, and R. J. Birgeneau, Phys. Rev. Lett. **74**, 964 (1995).

[37] N. P. Ong, Z. Z. Wang, J. Clayhold, J. M. Tarascon, L. H. Greene, and W. R. McKinnan, Phys. Rev. B **35**, 8807 (1987).

[38] Y. Fukuzumi, K. Mizuhashi, K. Takenaka, and S. Uchida, Phys. Rev. Lett. **76**, 684 (1996).

[39] C. Gros and R. Valenti, Ann. Phys. (Leipzig) **3**, 460 (1994).

[40] S. A. Trugman, Phys. Rev. Lett. **65**, 500 (1990).

[41] V. I. Belinicher, A. L. Chernyshev, and V. A. Shubin, Phys. Rev. B **53**, 335 (1996).

[42] D. Duffy and A. Moreo, Phys. Rev. B **52**, 15 607 (1995).

[43] D. M. King, Z.-X. Shen, D. S. Dessau, B. O. Wells, W. E. Spicer, A. J. Arko, D. S. Marshall, J. DiCarlo, A. G. Loeser, C. H. Park, E. R. Ratner, J. L. Peng, Z. Y. Li, and R. L. Greene, Phys. Rev. Lett. **70**, 3159 (1993).

[44] J. E. Hirsch and D. J. Scalapino, Phys. Rev. Lett. **56**, 2732 (1986).

[45] I. E. Dzyaloshinskii, Zh. Eksp. Teor. Fiz **93**, 1487 (1987) [Sov. Phys. JETP **66**, 848 (1987)].

[46] D. M. Newns, H. R. Krishnamurthy, P. C. Pattnaik, C. C. Tsuei, C. C. Chi, and C. L. Kane, Physica B **186–188**, 801 (1993).

[47] D. S. Marshall, D. S. Dessau, A. G. Loeser, C-H. Park, A. Y. Matsuura, J. N. Eckstein, I. Bozovic, P. Fournier, A. Kapitulink, W. E. Spicer, and Z.-X. Shen, Phys. Rev. Lett. **76**, 4841 (1996).

[48] Z.-X. Shen, W. E. Spicer, D. M. King, D. S. Dessau, and B. O. Wells, Science **267**, 343 (1995).

[49] G.-Q. Zheng, T. Kuse, Y. Kitaoka, K. Ishida, S. Ohsugi, K. Asayama, and Y. Yamada, Physica C **208**, 339 (1993).

[50] Y. Ohota, W. Koshibae, and S. Maekawa, J. Phys. Soc. Jpn. **61**, 2198 (1992).

[51] T. Tsuji, O. Narikiyo, and K. Miyake, Physica C **244**, 311 (1995).

[52] W. F. Brinkman and T. M. Rice, Phys. Rev. B **2**, 4302 (1970).